Development 137, 2551-2558 (2010) doi:10.1242/dev.046987

Oriented cell motility and division underlie early limb bud morphogenesis

Laurie A. Wyngaarden[1], Kevin M. Vogeli[2], Brian G. Ciruna[1,3], Mathew Wells[4], Anna-Katerina Hadjantonakis[5] and Sevan Hopyan[1,6,*]

SUMMARY

The vertebrate limb bud arises from lateral plate mesoderm and its overlying ectoderm. Despite progress regarding the genetic requirements for limb development, morphogenetic mechanisms that generate early outgrowth remain relatively undefined. We show by live imaging and lineage tracing in different vertebrate models that the lateral plate contributes mesoderm to the early limb bud through directional cell movement. The direction of cell motion, longitudinal cell axes and bias in cell division planes lie largely parallel to one another along the rostrocaudal (head-tail) axis in lateral plate mesoderm. Transition of these parameters from a rostrocaudal to a mediolateral (outward from the body wall) orientation accompanies early limb bud outgrowth. Furthermore, we provide evidence that *Wnt5a* acts as a chemoattractant in the emerging limb bud where it contributes to the establishment of cell polarity that is likely to underlie the oriented cell behaviours.

KEY WORDS: Wnt5a, Cell migration, Cell polarity, Limb bud, Morphogenesis, Oriented cell division, Mouse, Zebrafish, Chick

INTRODUCTION

The earliest morphological sign of vertebrate limb formation is an apparent thickening of the lateral plate mesoderm. Forelimb initiation occurs at a stage of development when roughly half of the somites have been laid down, while the rostrocaudal axis of the embryo, including the lateral plate, continues to elongate. Initially, the limb ridge is elongated and grossly symmetrical in the rostrocaudal axis (which corresponds to the anteroposterior axis of the limb). During the first day of outward (proximal to distal) growth, the limb bud acquires a stereotypical shape that is broader posteriorly than anteriorly and is relatively narrow in the dorsoventral axis. Some of the key molecular requirements for limb initiation and early outgrowth have been identified, and include T-box transcription factors (Agarwal et al., 2003; Ahn et al., 2002; Minguillon et al., 2005; Naiche and Papaioannou, 2003) and signalling by fibroblast growth factor 10 (Fgf10) (Min et al., 1998; Sekine et al., 1999). By contrast, the cellular dynamics and tissue mechanisms underlying formation of the initial limb ridge and remodelling of the early limb bud are not well understood.

Several cellular mechanisms that might underlie limb initiation have been proposed. Previous analysis in the chick demonstrated that the limb-forming region of the lateral plate mesoderm maintains a high proliferative rate, while that of the trunk region diminishes during early limb outgrowth (Searls and Janners, 1971). However, at least for the established limb bud, differential proliferation cannot fully explain outgrowth. Computer simulation of limb bud growth, based solely on the regional distribution of cell proliferation found in the bud (Fernández-Terán et al., 2006), fails to predict the generation of an appropriately shaped elongating limb bud, but rather predicts the generation of a relatively spherical morphology (Boehm et al., 2010). Therefore, anisotropic or oriented cell behaviours might contribute to limb bud outgrowth and the generation of its stereotypical shape.

Evidence for the presence of cell movement in the limb bud is found in both mouse and zebrafish models. In mature mouse limb buds at embryonic day (E) 11.0, four-dimensional time-lapse imaging revealed outward, rotatory movement of the surface ectoderm (Boot et al., 2008), although these studies were not at cellular resolution and neither mesoderm nor early stages were assessed. Lateral plate mesoderm cells lacking *tbx5* in zebrafish (Ahn et al., 2002) fail to enter the pectoral fin bud. Furthermore, *Fgfr1* mutant cells in mouse embryo chimaeras fail to populate the limb, in contrast to wild-type (WT) cells, which do (Ciruna et al., 1997; Saxton et al., 2000). It has also been shown that Fgf4, which is secreted by the apical ectodermal ridge (AER), can act as a chemoattractant (Li and Muneoka, 1999). An intriguing alternative mechanism is that Fgf might function to increase the liquid-like cohesiveness of mesoderm in the limb field (Damon et al., 2008; Heintzelman et al., 1978). This might cause the limb field to phase separate from the adjacent lateral plate mesoderm. In isolation, this property would cause the limb field mesoderm to be engulfed by the lateral plate. However, the lateral plate exhibits a unique active-rebound response that promotes limb bulging (Damon et al., 2008). Micromass culture data suggest that differential adhesiveness is an important mechanism that underlies the segregation of cells in the mature limb bud into proximodistal domains (Barna and Niswander, 2007).

Another signalling molecule that might contribute to cell movement during limb outgrowth is Wnt5a. The *Wnt5a* gene is expressed in the elongating tail bud and in the early ventral limb bud ectoderm, then shortly thereafter in the distal limb bud ectoderm and mesoderm, among other areas of outgrowth (Gavin et al., 1990; Yamaguchi et al., 1999). Mouse embryos lacking *Wnt5a* exhibit shortened rostrocaudal body axes and limbs (Yamaguchi et al., 1999). Wnt5a is able to cause directional cell movement in vitro by reorienting the cytoskeleton in response to a

[1]Program in Developmental and Stem Cell Biology, The Hospital for Sick Children, Toronto, M5G 1X8, Canada. [2]Departments of Anatomy and of Biochemistry and Biophysics, University of California, San Francisco, CA 94158, USA. [3]Department of Molecular Genetics, University of Toronto, M5S 1A8, Canada. [4]Department of Physical and Environmental Sciences, University of Toronto, M1C 1A4, Canada. [5]Developmental Biology Program, Sloan-Kettering Institute, New York, NY 10065, USA. [6]Division of Orthopaedic Surgery, The Hospital for Sick Children, University of Toronto, Toronto, M5G 1L5, Canada.

*Author for correspondence (sevan.hopyan@sickkids.ca)

Accepted 18 May 2010

chemokine gradient (Witze et al., 2008). It is conceivable that a similar mechanism might contribute to limb bud outgrowth in addition to the known positive effect of Wnt5a on mesoderm proliferation (Yamaguchi et al., 1999).

By contrast, it has been suggested that cell movement is a feature of limb formation only in lower vertebrates, and not in mouse or chick (Rallis et al., 2003). However, a direct survey of individual cell behaviours during early limb outgrowth in the mouse or chick has not previously been undertaken. The possibility that orientated cell division occurs during limb bud outgrowth has been addressed, although not systematically tested (Hornbruch and Wolpert, 1970). Here we utilise genetic, live-imaging and lineage-tracing techniques to directly survey the movements, shapes and division planes of mesodermal cells in mouse, chick and zebrafish embryos to define the morphogenetic mechanisms that generate the early limb bud and address whether equivalent cell behaviours drive this event across vertebrates. Our studies reveal the directional movement of mesoderm into the early limb bud, as well as spatially distinct biases in cell shape and cell division plane between the lateral plate and limb bud across species. A transition of these largely parallel parameters accompanies, and is likely to contribute to, early outgrowth of the bud. Cell polarity, which is partially conferred by *Wnt5a*, is likely to underlie these oriented cell behaviours.

MATERIALS AND METHODS

Embryo culture

CAG::H2B-EGFP (Hadjantonakis and Papaioannou, 2004) and *CAG::myr-Venus* (Rhee et al., 2006) transgenic mouse lines were used, and crossed with *Wnt5a*$^{-/-}$ mutants (Yamaguchi et al., 1999). E9.25-9.5 embryos [corresponding to late Theiler stage 14 (18-20 somites) to stage 15 (21-25 somites); Bard et al., 1998] were dissected and decapitated in DMEM containing 10% fetal calf serum. For live imaging, embryos were submerged just below the surface of optimised media (see Results) containing 25% DMEM and 75% rat serum. Cheese cloth or fragments of 1% agarose were used to position the lateral plate mesoderm and early limb bud directly against a coverslip at the bottom of a metallic confocal well, such that the entire depth of the tissue under study could be visualised. Time-lapse imaging experiments were performed for periods of up to 3 hours in a humidified chamber at 37°C in 5% CO_2. The presence of pyknotic nuclei disqualified live-imaging experiments from analysis.

Two transgenic zebrafish lines, *h2af/z:gfp* (Pauls et al., 2001) and *βactin:hras-egfp* (Cooper et al., 2005), were used. Embryos were cultured using Mesab (tricaine, Sigma) anaesthetic in egg water at 28°C for up to 3 hours in air. Some zebrafish embryos were cultured in egg water in the presence of 4 μM latrunculin A or its carrier 0.1% DMSO.

Image acquisition

Laser-scanning confocal data were acquired using a Zeiss LSM 510 META microscope system and a LiveCell culture chamber (Neue Biosciences). GFP and Venus fluorophores were excited using a 488 nm argon laser. For three-dimensional time-lapse experiments, a high frequency of mitoses and a lack of pyknotic nuclei in every acquired *z*-stack, as visualised directly with the aid of the *CAG::H2B-EGFP* and *h2af/z:gfp* reporters, confirmed good tissue health (Plusa et al., 2008). During the stages investigated in this study, there is normally little to no apoptosis in the mouse limb bud (Fernández-Terán et al., 2006). Therefore, the presence of any pyknotic nuclei disqualified data sets from analysis. Confocal images were acquired as *z*-stacks of *xy* images taken at 2-5 μm *z* intervals.

We focused on the two-dimensional coronal plane that is composed of the proximodistal (defined here as the *x*-axis) and rostrocaudal (or anteroposterior, defined as the *y*-axis) axes and did not record data in the dorsoventral (*z*) axis, as resolution along this axis is poor with current instrumentation and optimal acquisition for maintaining sample viability.

Lineage tracing

Chick embryos at Hamburger and Hamilton stage (HH) 15-17 were exposed through a window in the shell. Hand-pulled glass needles were used to deliver small spots of DiI to the lateral plate mesoderm. Embryos were photographed using a Leica MZ16 F stereomicroscope to document the position of the dye, and then cultured in ovo at 39°C until HH 20 prior to being rephotographed.

Zebrafish embryos were injected at the one-cell stage with DMNB-FITC for ubiquitous distribution and allowed to develop in the dark until 16 hours post-fertilisation (hpf). Cells in the lateral plate were then labelled through photo-activation of the FITC with a 365 nm laser focused through a 20× objective on a compound microscope. Embryos were allowed to develop until 28 hpf and were then immunostained against FITC to amplify the signal.

Chemotaxis assays

Acrylic beads were soaked for 1 hour in Wnt5a (1 mg/ml), Fgf8 (1 mg/ml), sonic hedgehog (Shh) (1 mg/ml), retinoic acid (RA) (10 μg/ml) (Helms et al., 1994), or carrier (PBS; DMSO for RA). HH 16 chick embryos were accessed in ovo through a window. The ectoderm overlying the lateral plate mesoderm was incised just enough to allow implantation of an acrylic bead into the mesoderm. Small spots of DiI were placed within 200 μm rostral and caudal to the bead for optimal sensitivity based on the findings of a previous chemotaxis assay (Li and Muneoka, 1999). Distance was measured directly from captured images using the scale bar. Embryos were photographed using a Leica MZ16 F stereomicroscope to document the position of the dye relative to the bead and then cultured in ovo at 39°C until HH 20, prior to being rephotographed. Maintenance of separation between the bead and the DiI was taken to imply a lack of chemoattraction, as was seen with all carrier-soaked beads. Approximation of previously separated DiI to the bead in the form of a contiguous streak was taken to imply chemoattraction of mesoderm to the bead.

Image processing

Particle image velocimetry (PIV; DaVis, LaVision, Göttingen, Germany) was used to determine bulk tissue motion based on the trajectory of fluorescent nuclei over successive time-lapse frames in two dimensions.

Cell polarity

Paraffin-embedded sections were stained against GM130 (Golga2), a Golgi matrix protein, and counterstained with the nuclear marker DAPI. The angle, from 0-359°, at which the Golgi lay with respect to the centre of the nucleus was measured for individual cells using the rostrocaudal embryo axis as the 0/180° line of reference. Confocal microscopy was used to obtain multiple *z*-stacks through the entire specimen under investigation. The nucleus-Golgi angles were measured for all cells while avoiding duplication by selecting *z*-stacks separated by one cell diameter. Measurements were grouped into twelve segments of 30° and were represented on a polar plot.

Orientation of cell division

Time-lapse movies of *CAG::H2B-EGFP* and *h2af/z:gfp* transgenic mouse and zebrafish limb buds imaged in the coronal plane were inspected frame-by-frame using Volocity software (Improvision). Confocal *z*-stacks, together encompassing the entire depth of the tissue under study, were assessed individually. Care was taken not to record duplicate mitoses on adjacent *z*-stacks by ensuring that they were separated by one cell depth. Two regions were analysed separately: lateral plate mesoderm medial to where the limb bud protrudes beyond the trunk, and the limb bud lateral to that line. Tracing paper was used to draw a line precisely representing the metaphase-to-telophase transition of every single mitosis identified. Angles of these lines were measured from 0-180° using a compass with reference to the rostrocaudal axis of the embryo as derived from low-magnification images, with 0 representing the rostral end. The planes of cell division were grouped into six segments of 30° and were represented on a polar plot with segments shaded symmetrically about the centre. Segment length was used to denote the proportion of divisions within that range. This methodology is capable of detecting a bias in cell division along the rostrocaudal and proximodistal axes, but not the dorsoventral axis.

RESULTS

The trajectory of tissue movement into the mouse early limb bud

To characterise cell movements during early limb bud outgrowth, we first established a system facilitating the ex utero development of intact lateral plate and early limb bud mesoderm in which those tissues could be live imaged. Transgenic *CAG::H2B-EGFP* mouse embryos (Hadjantonakis and Papaioannou, 2004) were used because localisation of the H2B-GFP fusion reporter to chromatin facilitates the visualisation of nuclei during all phases of the cell cycle, such that cells can be segmented and individually tracked in four dimensions (three-dimensional time-lapse). We optimised 3-hour static culture conditions of decapitated E9.0-9.5 (18-25 somites) mouse embryos by testing various media and rat serum concentrations. Using the quality of extracted ribosomal RNA bands as a readout, we determined that in a 5% CO_2 environment maintained at 37°C, 75% rat serum supplemented with DMEM provided optimal ex utero development of static samples in a chamber resting on the microscope stage (see Fig. S1A in the supplementary material). We confirmed that short-term culture under these conditions did not result in increased cell death as assessed by LysoTracker Red staining (see Fig. S1B in the supplementary material), nor in dysmorphology of the limb bud (see Fig. S1C in the supplementary material). Using this formulation coupled with rapid dissection and short-term (up to 3 hours) time-lapse imaging experiments, pyknotic nuclei (a sign of cell necrosis, see Materials and methods) were rarely observed in *CAG::H2B-EGFP* transgenic tissues during live-image data acquisition.

As forelimb and hindlimb development might be subject to distinct kinetics, we chose to focus our studies on the forelimb. During Theiler stage 14 (~E9.0-9.25, 18-20 somites) the prospective mouse forelimb field appears as a barely perceptible thickening of lateral plate mesoderm between somites 8 and 12. Live imaging at this site revealed tissue movement in a rostral-to-caudal direction relative to somite boundaries (n=8 embryos studied) (Fig. 1A; see Movie 1 in the supplementary material). This finding explains previous fate-mapping (Chaube, 1959) and *Tbx5* gene expression (Agarwal et al., 2003; Ahn et al., 2002; Zhao et al., 2009) studies that suggest a caudal progression of the prospective forelimb-forming region of the lateral plate mesoderm relative to the somites, prior to overt limb morphogenesis.

At Theiler stage 15 (~E9.25-9.5, 21-25 somites), lateral plate mesoderm was seen entering the early forelimb bud at an oblique angle from rostral positions (Fig. 1B,C), and laterally from more central positions relative to the limb bud (Fig. 1D; see Movie 2 in the supplementary material). The relative velocity of movement gradually increased from proximal to distal within the bud (Fig. 1D,E). This finding suggests that velocity is additive within the bud, and that the substrate for movements is the neighbouring cells themselves. Movement into the limb bud from caudal positions relative to the bud was not observed. Rather, tissue in the posterior aspect of the limb bud demonstrated rotational movement, such that cells at the posterior edge moved slightly back towards the embryo (n=10) (Fig. 1E; see Movie 2 in the supplementary material). This pattern of movement is partially analogous to the rotational motion of later limb ectoderm (Boot et al., 2008) and to polonaise movements that occur during primitive streak formation (Cui et al., 2005; Voiculescu et al., 2007), suggesting that rotation of tissue commonly accompanies longitudinal growth during development. In summary, these data indicate that lateral plate mesoderm cells migrate into the early mouse limb bud, and do so primarily from rostral and lateral positions (Fig. 1F).

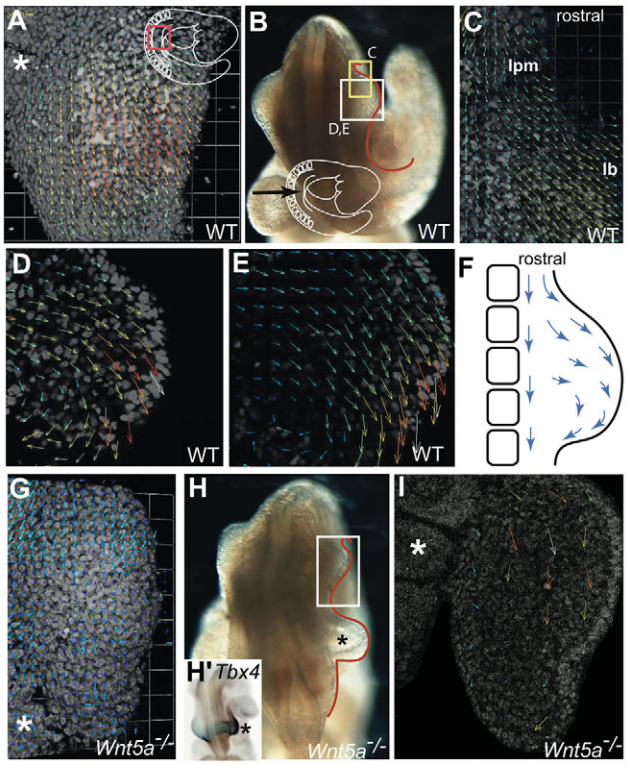

Fig. 1. Mesoderm trajectories during mouse early limb outgrowth. For vector velocity fields (VVFs), longer arrow length and red end of the spectrum correlate with higher relative velocity within a given experiment. (**A**) VVF of lateral plate mesoderm adjacent to somites 8-12 of a *CAG::H2B-EGFP* transgenic embryo at late Theiler stage 14 (E9.0-9.25, 18-20 somites), just prior to limb outgrowth. Rostral-to-caudal tissue movement relative to a stationary somite boundary (asterisk) is evident. Inset depicts field of view. (**B**) Dorsal view of early forelimb buds of a Theiler stage 15 (E9.25-9.5, 21-25 somites) wild-type (WT) embryo. The inset and arrow depict the direction of view; the orange line indicates the margin of the right-hand side lateral plate mesoderm. The hindlimb bud is beyond the field of view. The boxed regions indicate the field of view in C-E. (**C**) VVF of the anterior margin of a early WT limb bud at Theiler stage 15. Mesoderm moves obliquely from lateral plate mesoderm (lpm) toward the limb bud (lb). (**D**,**E**) Separate *z*-stacks of a Theiler stage 15 WT forelimb bud. Within the early limb bud, mesoderm moves in a posterodistal direction. Tissue near the posterior margin rotates in a proximal direction. (**F**) Schematic depiction of regional tissue vectors during early limb outgrowth. (**G**) Lateral plate mesoderm of *Wnt5a*$^{-/-}$*;CAG::H2B-EGFP*$^{Tg/+}$ at Theiler stage 14 lacks the coordinated movement seen in the WT embryo (A). Asterisk overlies somite. (**H**) The long-body axis and lateral plate mesoderm of a *Wnt5a*$^{-/-}$*;CAG::H2B-EGFP*$^{Tg/+}$ embryo at Theiler stage 15 are shortened as compared with the WT embryo (B). The orange outline delineates the truncated lateral plate mesoderm and the hindlimb bud (*), which is in abnormally close proximity to the forelimb bud. (**H′**) Expression of *Tbx4* by in situ hybridisation confirms that the bulge close to the forelimb is indeed the hindlimb. The forelimb (boxed region) is shown in I. (**I**) Tissue movement into the early *Wnt5a*$^{-/-}$*;CAG::H2B-EGFP*$^{Tg/+}$ limb bud is evident, albeit at a lower velocity, compared with WT embryos (see text).

Wnt5a has been implicated in the regulation of cell polarity and directional cell movement in a number of contexts, including the morphogenesis of early mesoderm (Sweetman et al., 2008; Witze et al., 2008). *Wnt5a* mutant mice exhibit severe shortening of the body axis and limbs (Yamaguchi et al., 1999). To determine

whether this mutant phenotype might be due, in part, to a cell migration defect, we used the *CAG::H2B-GFP* reporter to live image *Wnt5a*$^{-/-}$ embryos. At Theiler stage 14, lateral plate mesoderm cells of *Wnt5a*$^{-/-}$ embryos lacked the rostral-to-caudal movement seen in WT littermates (*n*=5) (Fig. 1G; see Movie 3 in the supplementary material). At Theiler stage 15, a corresponding shortening of the lateral plate mesoderm (and entire long-body axis) was clearly evident (Fig. 1H). This shortening is underscored by the unusual proximity of the hindlimb bud field (as identified by expression of *Tbx4*, a specific marker of the hindlimb) to the forelimb (Fig. 1H′). Cells in the early *Wnt5a*$^{-/-}$ forelimb bud moved with a vector comparable to that of WT littermates, albeit at a reduced velocity (Fig. 1I; see Movie 4 in the supplementary material). The mean velocity of randomly selected cells individually traced frame-by-frame from *z*-stacks midway through the dorsoventral axis for 1.5 hours in WT embryos was 20.2 μm/hour (s.d.=2.6), compared with 10.8 μm/hour (s.d.=2.3) in the mutants, (P<0.0001, *n*=20 cells traced in three embryos each). Therefore, these data suggest that *Wnt5a* is necessary to maintain the normal velocity of mesoderm cell movements.

Tissue movement in chick

To cross-validate our directional movement findings from the mouse embryo, we studied tissue displacements in the chick embryo by lineage tracing. The chick wing bud arises from lateral plate mesoderm adjacent to somites 18-22 at HH 16 (26-28 somites total) (Chaube, 1959). HH 15-17 chick embryos were labelled with DiI and cultured in ovo at 39°C until HH 20 (40-43 somites). Lateral plate mesoderm labelled in the rostral portion of the wing bud-forming region, adjacent to somites 17 and 18, left a trail of dye entering the early wing bud in a caudal and lateral direction (*n*=10) (Fig. 2A,B). Mesoderm that was labelled more centrally and inferiorly, adjacent to somites 19-21, resulted in a more directly lateral trail of DiI entering the bud (*n*=6) (Fig. 2C,D). Tissue caudal to somite 21 was not found to enter the wing bud, but rather became displaced just caudal to the bud (*n*=7; data not shown). The linear displacement of dye that we observed, as opposed to the displacement of intact spots, could result from a number of mechanisms, including directed cell migration and oriented cell division. Nonetheless, the pattern of mesoderm movement into the early wing bud, however, was similar to that of the mouse limb bud.

Wnt5a as a chemoattractant

To identify candidate molecules that might function to draw mesoderm into the early limb field, we performed chemotaxis assays in chick embryos. We tested Wnt5a, Fgf8, sonic hedgehog (Shh) and retinoic acid (RA). Wnt5a is expressed in the early ectoderm and distal mesenchyme of the nascent limb bud (Gavin et al., 1990), whereas Fgf8 is expressed by the AER (Crossley and Martin, 1995). Shh is expressed in the posterior limb bud mesoderm (Riddle et al., 1993), and RA is expressed in lateral plate mesoderm prior to, and during, limb initiation, and is necessary for forelimb induction (Zhao et al., 2009). Acrylic beads were soaked in protein or carrier for 1 hour prior to implantation into HH 16 chick embryo lateral plate mesoderm. Spots of DiI were placed rostral and caudal within 200 μm of the bead for optimal sensitivity of the assay (Li and Muneoka, 1999), and the position of these spots relative to the bead was documented. Following overnight incubation in ovo, the position and configuration of the DiI relative to the bead was again documented. Beads soaked in Wnt5a, but not PBS, frequently became surrounded by DiI that was contiguous

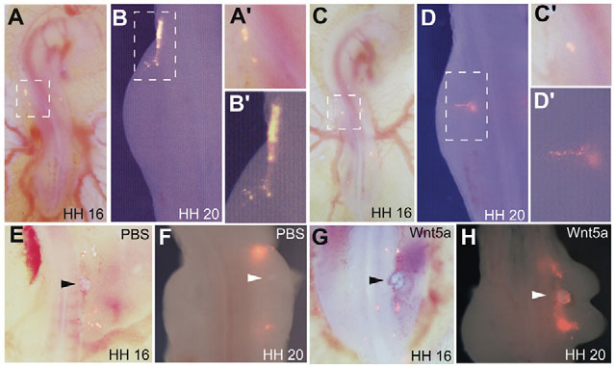

Fig. 2. Regional lineage of chick lateral plate mesoderm during early wing bud outgrowth. Merged bright-field and fluorescent images. (**A**,**A′**) Chick embryo labelled with spots of DiI (orange) at HH 16 (26-28 somites) at the start of wing bud outgrowth and cultured in ovo. The rostral-most spots on the left side are adjacent to somites 17/18. (**B**,**B′**) In the same embryo at HH 20, DiI-labelled tissue has become displaced into the wing bud. Streaks of DiI suggest caudal-lateral oblique movement of mesoderm into the anterior wing bud from a rostral position. (**C-D′**) Lineage tracing in another embryo with images taken before (C,C′) and after (D,D′) culture in ovo. DiI spots adjacent to somites 19/20 at HH 16/17 (C,C′) were displaced in a linear fashion by HH 20, heading directly lateral (D,D′). These findings are consistent with the movements observed in the mouse embryo, as shown in Fig. 1. (**E-H**) Pre- and post-culture images showing that chemoattraction of DiI-labelled mesoderm is not apparent toward a bead (arrowheads) soaked in PBS (E,F), but is apparent toward a bead soaked in Wnt5a protein in PBS (G,H).

with the previously distinct spot of dye (P=0.04, Fisher's exact test) (Table 1, Fig. 2E-H). Neither carrier alone, nor any of the other proteins tested, exhibited evidence of chemotaxis. These data suggest that Wnt5a acts as a chemoattractant of mesoderm. Our observations are consistent with similar findings in the developing mouse palate (He et al., 2008).

Tissue movement in zebrafish

We extended our tissue movement analyses to zebrafish (*Danio rerio*) to establish whether the early mechanisms of budding are conserved despite the divergent structural features of the mature limb and fin. The zebrafish pectoral fin bud becomes morphologically distinct from lateral plate mesoderm adjacent to somites 2 and 3 at 24 hpf (26 somites). To localise the region of the lateral plate mesoderm that gives rise to the pectoral fin bud, we performed lineage tracing. Ubiquitously distributed, but non-emitting fluorescein (DMNB-FITC), was uncaged in lateral plate mesoderm adjacent to specific somites using a focused laser at 18 hpf (18 somites), prior to fin initiation (Fig. 3A). Embryos developed until 28 hpf (30 somites) and were then immunostained

Table 1. Wnt5a acts as a chemoattractant of mesoderm

Bead	Chemoattraction	No effect
PBS	0	5
Fgf8 in PBS	0	14
Wnt5a in PBS	11	8
Shh in PBS	0	19
DMSO	0	14
Retinoic acid in DMSO	0	14

Shown are the number of beads exhibiting evidence of chemoattraction in chemotaxis assays performed in chick embryos.

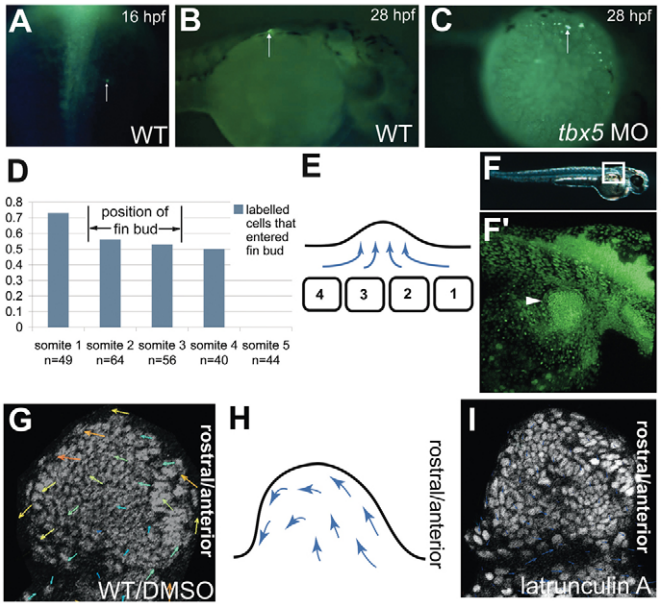

Fig. 3. Lineage and movement of mesoderm during early pectoral fin development in zebrafish. (**A**) Fluorescein uncaged in the lateral plate mesoderm (arrow) at 16 hpf (18 somites). (**B**) By 28 hpf (30 somites), in the same embryo as in A, focal fluorescence is found in the early fin bud (arrow). (**C**) In *tbx5* morpholino (MO) knockdown embryos, a fin bud fails to form and labelled tissue becomes scattered throughout the mesoderm (arrow). (**D**) Summary of lateral plate lineage-tracing experiments. Mesoderm adjacent to somites 1 to 4, but not 5, contributes to the pectoral fin bud. (**E**) Since the pectoral fin bud arises adjacent to somites 2 and 3, we infer that lateral plate mesoderm condenses during fin initiation. (**F**,**F′**) Field of view (boxed) and position of a maturing pectoral fin bud at 44 hpf (arrowhead), positioned as in G-I. (**G**) VVF of an *h2af/z:gfp* transgenic embryo at 44 hpf. (**H**) Schematic representation of tissue movements in the maturing (35-45 hpf) fin bud. The movements are comparable to those of the mouse limb bud, taking into account the different orientation of the two buds with respect to the embryo body. (**I**) VVF of a 44 hpf embryo treated with 4 μM latrunculin A. Tissue motion is halted (but not with 0.1% DMSO carrier) as demonstrated by the lack of arrows under PIV analysis.

against FITC. We found that cells labelled in the lateral plate adjacent to somites 1-4, but not those adjacent to somite 5, contributed to the mature pectoral fin bud (Fig. 3B,D). For validation of our lineage-tracing method, we performed the same experiment in the presence of morpholinos against *tbx5* that are known to produce deficient pectoral fins. As expected (Ahn et al., 2002), mesoderm in these embryos that was labelled adjacent to somites 1-4 became scattered, rather than focused, in the limb bud (Fig. 3C). Our lineage-tracing observations suggest that lateral plate mesoderm condenses during formation of the pectoral fin (Fig. 3E). In contrast to the mouse embryo, in which primarily rostral lateral plate tissue migrates into the limb bud, zebrafish lateral plate tissue migrates from both rostral and caudal positions to enter the early bud.

To assess cell movements in the more mature pectoral fin bud, but prior to cartilaginous condensation, we live imaged *h2af/z:gfp* (Pauls et al., 2001) transgenic zebrafish embryos. With the embryo in the sagittal plane, views of the broad two-dimensional proximodistal-anteroposterior surface of the pectoral fin bud, comparable to those of the mouse forelimb bud, were achieved (Fig. 3F,F′). Limited cell movements were seen between 28 and 40 hpf (see Movie 5 in the supplementary material). From 40 to 45 hpf, fin mesoderm cells could be seen to move in a rotatory fashion, from proximal-anterior to distal-posterior (n=16) (Fig. 3G; see Movie 6 in the supplementary material). This movement was analogous to those in the mouse limb bud at Theiler stage 15 (Fig. 3H), taking into account the different orientation of the limb and fin buds. Tissue motion was abolished in the presence of 4 μM latrunculin A, but not 0.1% DMSO carrier (n=4) (Fig. 3I; see Movie 7 in the supplementary material), indicating that actin-based mechanisms are required for cell movement.

Regional differences in cell shape and polarity

Having shown that the movement of cells is regionally distinct in the forelimb-forming region of each organism, we sought to establish whether mesoderm cells in these regions exhibit a distinct shape and orientation. We performed live imaging of *CAG::myr-Venus* transgenic mice (Rhee et al., 2006) and *βactin:hras-egfp* (Cooper et al., 2005) transgenic zebrafish. These transgenic reporters illuminate the cell perimeter, avoiding potential artefactual changes in cell morphology that might be associated with tissue fixation. Multiple *z*-stacks encompassing the entire depth of the relevant tissue were taken in the coronal plane. By imaging multiple planes and identifying the distinct morphological characteristics of the single-cell layer of ectoderm (Fig. 4), we ensured that only mesoderm was analysed. Regional differences in mesoderm cell shape were identified in both mouse and zebrafish. Mouse lateral plate mesoderm cells at Theiler stage 14 (n=11) and those just medial to the early limb bud at Theiler stage 15 (n=9) displayed elongated shapes that ran parallel to the rostrocaudal axis of the embryo body (Fig. 4A,C). However, in *Wnt5a*$^{-/-}$ mutants, elongated cell shapes were not apparent at either stage (n=7 and 4, respectively) (Fig. 4B,D). WT (n=9) and *Wnt5a*$^{-/-}$ mutant (n=9) limb bud cells lateral to the trunk at Theiler stage 15 exhibited isotropic shapes without a longitudinal bias (Fig. 4A-F). Little to no intervening space between cells was evident by live imaging (Fig. 4A-F).

To test whether mesoderm cells exhibit polarity that corresponds to their direction of movement, we determined the location of the Golgi apparatus relative to the nucleus. The Golgi apparatus is commonly located near the leading edge of a motile cell (Nabi, 1999). At Theiler stage 14 (20 somites), we identified a caudal and lateral bias in the position of the Golgi in WT mesoderm cells (n=3) (Fig. 4G,I). However, in *Wnt5a*$^{-/-}$ mutant mesoderm, this bias was not apparent (n=3, P<0.05, χ^2 test) (Fig. 4H,J). These findings correlate with the direction of mesoderm movement in WT embryos as well as with the diminished movements seen in *Wnt5a*$^{-/-}$ mutants, and suggest that cell polarity is required for directed cell movements.

In zebrafish, lateral plate cells at the base of the pectoral fin bud also exhibited a longitudinal bias parallel to the rostrocaudal axis of the embryo (n=6) (Fig. 4K). Most of the cells within the fin bud were isotropic between 35 and 45 hpf, as in the mouse bud, but cells at the proximal-anterior portion of the 40-45 hpf fin bud displayed a distinctive mediolateral longitudinal orientation, parallel to the proximodistal axis of the fin bud and perpendicular to the rostrocaudal embryo axis (n=10) (Fig. 4L,M). Silencing of the *βactin:hras-egfp* transgene resulted in mosaic reporter expression and facilitated the visualisation of individual cell morphologies. We observed actin-rich protrusions pointing posterodistally from the distal end of the elongated cells (Fig. 4K,M). These protrusions were likely to be filopodia, localised to the leading edge of cells and extending in the direction of movement.

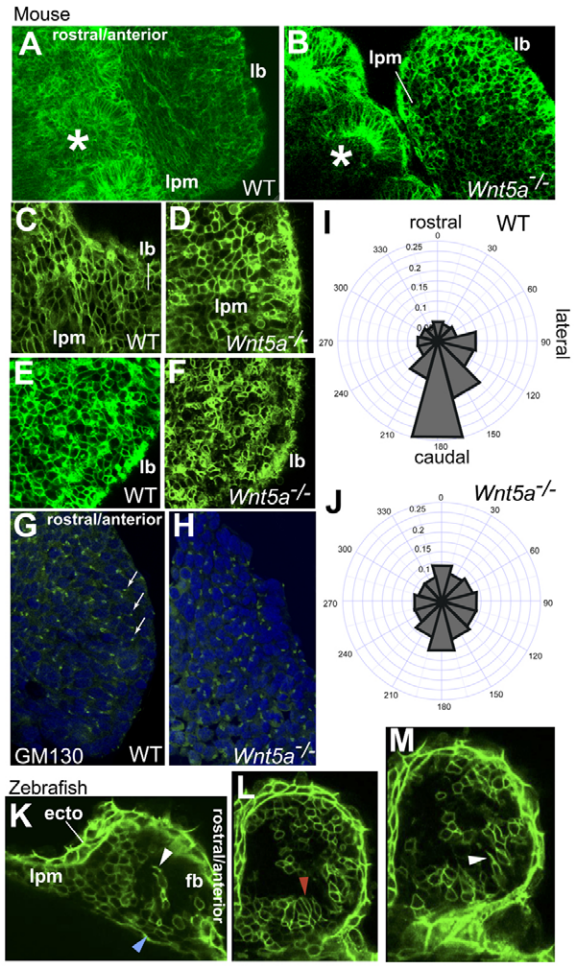

Fig. 4. Regional differences in cell shape during early limb bud outgrowth. (**A-F**) Theiler stage 15 (21-25 somites) *CAG::myr-Venus* transgenic mouse embryos imaged live using a confocal microscope. Rostral positions are towards the top of the images. Somites, which contain cells of distinctive shape for comparison, are indicated by asterisks (A,B). WT lateral plate mesoderm (lpm) cells adjacent to the early limb bud are oriented longitudinally, parallel to the rostrocaudal axis of the embryo. This is observed as longitudinal streaking adjacent to the somites in A, and anteromedial to the early limb bud in C. Cells within the early WT limb bud (lb) are isotropic (A,C,E). By contrast, cells in *Wnt5a*$^{-/-}$ littermates (B,D,F) are isotropic in both the lateral plate and the limb bud. This finding correlates with the shortening and relative lack of tissue movement observed in *Wnt5a*$^{-/-}$ lateral plate mesoderm. (**G**,**H**) GM130 (Golga2) stain (green) highlights the location of the Golgi relative to nuclei (DAPI, blue). In Theiler stage 14 embryos (20 somites), Golgi are commonly found caudal and lateral to corresponding nuclei in the WT forelimb mesoderm field (arrows), but not in *Wnt5a*$^{-/-}$ mutants. Since Golgi are found at the leading edge of motile cells, these data correlate well with the direction of tissue motion in WT embryos, and the lack of movement of *Wnt5a*$^{-/-}$ mesoderm demonstrated in Fig. 1. (**I**,**J**) Polar plots summarising Golgi angle in relation to the nuclear centre, with embryonic reference marks as shown. (**K-M**) Separate *z*-stacks of a live *βactin:hras-egfp* transgenic zebrafish fin bud at 42 hpf. Lpm cells at the base of the fin bud (blue arrowhead, K) are elongated, parallel to the rostrocaudal axis of the embryo. Most cells in the fin bud are isotropic. However, cells in the proximal-anterior region of the fin bud are elongated, with an anteroproximal-to-posterodistal long axis, parallel to their direction of movement (red arrowhead, L). Some of these cells exhibit protrusions at their posterodistal tip (white arrowheads, K,M). ecto, ectoderm; lpm, lateral plate mesoderm; lb, limb bud; fb, fin bud.

Our data revealed parallels between cell orientation and the direction of tissue movement. A transition of cell behaviours is likely to involve active remodelling of the cytoskeleton because filopodia and Golgi localise to the leading side of mesoderm cells and latrunculin treatment impairs cell movement. The lack of apparent intercellular matrix seen by live imaging supports the proposal that the substrate upon which motion occurs is the cells themselves. Cell division might therefore be capable of influencing tissue motion.

Regional differences in the orientation of cell division

We sought to integrate data on cell division planes with our other findings. Time-lapse images of *CAG::H2B-EGFP* and *h2af/z:gfp* transgenic mouse and zebrafish buds, respectively, captured in the coronal plane were inspected frame by frame. Analysis of individual *z*-stacks facilitated the identification of mitotic planes (see Movie 8 in the supplementary material). The angle of the metaphase-to-telophase transition of every mitosis identified throughout a given specimen was measured with respect to the rostrocaudal axis (Fig. 5A).

In both mouse and zebrafish embryos, we found evidence for spatially distinct preferences in cell division planes. In lateral plate mesoderm at Theiler stage 14, the preferred plane of division was parallel to the rostrocaudal axis of the embryo (n=2 embryos, 61 mitotic angles measured; Fig. 5B). This bias was similar in lateral plate tissue medial to the early limb bud at Theiler stage 15 (n=2, 66 mitoses; Fig. 5C). In the early bud itself, a bias in the plane of cell division was identified perpendicular to the long axis of the embryo (n=2, 224 mitoses; Fig. 5D). The distribution of division planes was significantly different between WT lateral plate mesoderm and limb bud (P=0.007, χ^2 test). Cell division planes in *Wnt5a* mutant lateral plate mesoderm lacked the distinct orientation bias of WT embryos (n=2, 50 mitoses, P=0.05; Fig. 5E). However, in the *Wnt5a* mutant limb bud, there remained evidence of a bias in division plane largely perpendicular to the long axis of the embryo, similar to that of WT embryos (n=2, 59 mitoses, P=0.9; Fig. 5F).

Zebrafish embryos demonstrated similarities in cell division planes to mouse embryos. At 35 hpf, lateral plate mesoderm cells divided with a bias similar to that of mice (n=2, 24 mitoses; Fig. 5G), whereas fin bud cell divisions were more strikingly biased perpendicular to the embryo long axis (n=2, 30 mitoses, P=0.02; Fig. 5H). By 44 hpf, a preferred plane of cell division was no longer apparent in the lateral plate as compared with 35 hpf embryos (n=2, 20 mitoses, P=0.3; Fig. 5I). A cell division bias did persist in the 44 hpf fin bud, where it was comparable to that of 35 hpf embryos (n=2, 70 mitoses, P=0.6; Fig. 5J). Collectively, these data indicate that distinct preferences in cell division plane occur between lateral plate mesoderm and the early limb bud.

DISCUSSION

We have investigated the individual cell behaviours driving the tissue-scale morphogenetic mechanisms by which the vertebrate limb bud arises. Our findings challenge the notion that cell movement is a feature of only lower vertebrate early limb outgrowth (Rallis et al., 2003). Our data explain the previously observed caudal displacement of lateral plate mesoderm (Chaube, 1959) and of the *Tbx5* expression domain that marks the forelimb field prior to initiation (Agarwal et al., 2003; Zhao et al., 2009). Importantly, cell motion and division planes are reoriented during early limb outgrowth. Taken together with previous fate mapping

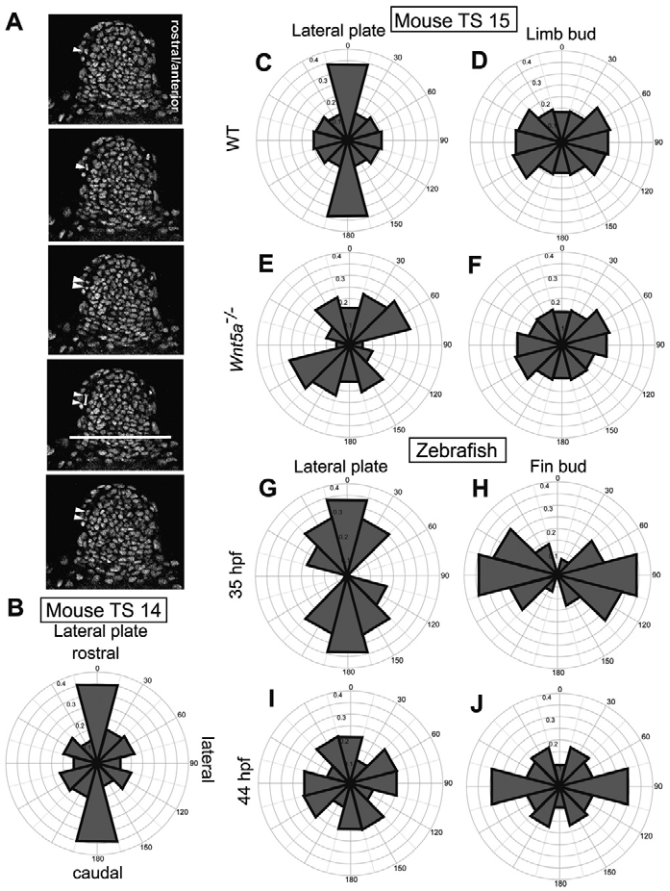

Fig. 5. Evidence for regionally localised oriented cell division during early limb development in mouse and zebrafish. (**A**) Method of measuring cell division angle. *h2af/z:gfp* transgenic zebrafish chromatin undergoing mitosis (arrowheads) is visualised on successive frames. The angle of a line joining the daughter chromatin centres at telophase is measured with reference to the longitudinal axis of the lateral plate mesoderm (fourth frame down). The level at which the limb bud protruded beyond the lateral plate was selected as the boundary between these two regions on every individual *z*-stack (long white line, fourth frame down). Every mitotic angle visualised on all *z*-stacks, together encompassing the entire limb bud, was measured over the whole duration of each time-lapse experiment. (**B-J**) Polar plot representations of cell division planes in which the rostrocaudal axis is defined at 0/180°, and the lateral and future distal axis of the limb bud is defined at 90°. The proportion of cell divisions in each 30° segment is represented by the length of the segment. (B) During mouse Theiler stage 14 (18 somites), lateral plate mesoderm adjacent to somites 8-12 exhibits a preferential plane of cell division that is parallel to the rostrocaudal embryo axis. At Theiler stage 15 (21-25 somites), although the same preferential plane of division is found in the lateral plate (C), cells in the early limb bud exhibit a different orientation of division that is perpendicular to the rostrocaudal axis, but parallel to the direction of bud outgrowth (D). In *Wnt5a*$^{-/-}$ mutants, orientation of cell division in the lateral plate is less apparent (E), although some orientation in the limb bud is evident (F). This finding correlates with the severe shortening and lack of tissue movement in the lateral plate mesoderm of *Wnt5a*$^{-/-}$ mutants, whereas budding of the limbs takes place with evident cell movement, as seen in Fig. 1. In zebrafish at 35 hpf, the orientation of cell division is similar to that of the mouse embryo (G), although more pronounced in the limb bud (H). By 44 hpf, orientation of cell division in the lateral plate is lost (I), while it persists in the fin bud (J).

of the later limb bud (Saunders, 1948; Vargesson et al., 1997) and genetic studies (Hasson et al., 2007; Naiche and Papaioannou, 2007; Ros et al., 1996), our results suggest that limb initiation and subsequent outgrowth represent distinct lateral plate-dependent and -independent phases of development.

Our comparative analyses reveal that cell movement occurs similarly in the mouse and chick. Mesoderm movement also occurs during early fin outgrowth, albeit in a different pattern that later becomes analogous to that of the mouse. Our data confirm that the apparent condensation of the *tbx5* expression domain during zebrafish pectoral fin initiation (Ahn et al., 2002) is secondary to cell movement, rather than to the loss and gain of expression among different cell populations. Differences in tissue movement during early forelimb outgrowth between the mouse and zebrafish might be attributable to differences in the position of the limb bud relative to the active site of rostrocaudal axis elongation at the tail end. In zebrafish, the posterior growing end of the embryo is, in relative terms, further away from the pectoral fin field, and the lateral plate mesoderm adjacent to the pectoral fin bud does not exhibit caudal-ward motion. The pre-existing caudal-ward vector adjacent to the mouse forelimb field is likely to influence cell movements into the early bud.

An active transition of cell polarity might provide the necessary coordinate behaviour that underlies initial bud outgrowth. We found that the oriented migration and division of mesoderm cells are linked. Disruption of cell polarity in the *Wnt5a* mouse mutants simultaneously resulted in the loss of longitudinal cell organisation, of oriented cell division and of directional movement. Although multiple forces, such as oriented cell division and directional cell movement, are likely to contribute to limb budding, these *Wnt5a* mutant data suggest that all such behaviours result from positional polarity possessed by mesoderm cells.

Our data are consistent with a model in which Wnt5a is involved both in establishing mesodermal cell orientation and in signalling the transition of cell polarity that is necessary to generate a limb bud. Expression of *Wnt5a* in the elongating tail bud is likely to contribute to the orientation of cells in the lateral plate mesoderm. By virtue of a new expression domain in the nascent limb field (Gavin et al., 1990), *Wnt5a* is likely to provide a repolarisation cue for mesodermal cells to move toward the new Wnt5a source. There are likely to be redundant factors contributing to this transition, as the limb bud was not as strongly affected as the lateral plate mesoderm in the absence of *Wnt5a*. A subset of the numerous Wnt and Frizzled genes that are expressed in the limb bud (Summerhurst et al., 2008) might perform this function, among other candidates.

Although the mechanism linking cell polarity with directional movement through cytoskeletal changes in response to Wnt5a has been explored in depth (Witze et al., 2008), the relationship of oriented division to directional movement remains unclear. We speculate that cell division generates a force that is capable of influencing the direction of movement of neighbouring cells in early mesoderm, where they are closely apposed. Although Fgf8 was not found to be a chemoattractant in our assay, it is likely to facilitate the entry of cells into the nascent limb bud by rendering the limb field mesoderm more fluid in nature (Damon et al., 2008) and by promoting cell survival (Sun et al., 2002). Directional movement and increased rates of proliferation also explain why the limb field, which exhibits higher tissue cohesiveness, is not engulfed by the lateral plate mesoderm. Our data therefore suggest that multiple mechanisms contribute to early limb bud outgrowth. Improvements in our ability to visualise and measure physical

forces in living embryos will facilitate further dissection of the nature and complexity of the morphogenetic mechanisms that generate the limb bud.

Acknowledgements
We thank Dr Terry P. Yamaguchi for *Wnt5a* mutant mice; Dr Jacek Topczewski and the late Dr José A. Campos-Ortega for *βactin:hras-egfp* and *h2af/z:gfp* transgenic zebrafish lines, respectively; Drs Gail Martin and Didier Stainier for guidance and review of the manuscript; Drs Sean Egan, Chi-chung Hui, Janet Rossant, James Sharpe, Patrick Tam, Rudolph Winklbauer and Yogiro Yamanaka for helpful discussions and review of the manuscript. This work was supported in part by Research Grant 5-FY07-652 from the March of Dimes Birth Defects Foundation and by a Pediatric Orthopaedic Society of North America Angela Kuo Young Investigator Award (to S.H.). K.M.V. was supported by an NSF Predoctoral fellowship and his work in the Martin and Stainier labs was supported by the NIH. Work in B.G.C.'s laboratory is supported by The Terry Fox Foundation. Work in M.W.'s laboratory is supported by NSERC and CFI. Work in A.-K.H.'s laboratory is supported by the NIH (RO1-HD052115 and RO1-DK084391) and NYSTEM. Deposited in PMC for release after 12 months.

Competing interests statement
The authors declare no competing financial interests.

Supplementary material
Supplementary material for this article is available at
http://dev.biologists.org/lookup/suppl/doi:10.1242/dev.046987/-/DC1

References

Agarwal, P., Wylie, J. N., Galceran, J., Arkhitko, O., Li, C., Deng, C., Grosschedl, R. and Bruneau, B. G. (2003). Tbx5 is essential for forelimb bud initiation following patterning of the limb field in the mouse embryo. *Development* **130**, 623-633.
Ahn, D. G., Kourakis, M. J., Rohde, L. A., Silver, L. M. and Ho, R. K. (2002). T-box gene tbx5 is essential for formation of the pectoral limb bud. *Nature* **417**, 754-758.
Bard, J. L., Kaufman, M. H., Dubreuil, C., Brune, R. M., Burger, A., Baldock, R.A. and Davidson, D. R. (1998). An internet-accessible database of mouse developmental anatomy based on a systematic nomenclature. *Mech. Dev.* **74**, 111-20.
Barna, M. and Niswander, L. (2007). Visualization of cartilage formation: insight into cellular properties of skeletal progenitors and chondrodysplasia syndromes. *Dev. Cell* **12**, 931-941.
Boehm, B., Westerberg, H., Lesnicar-Pucko, G., Raja, S., Rautschka, M., Cotterell, J., Swoger, J. and Sharpe, J. (2010). The role of spatially-controlled cell proliferation in limb bud morphogenesis. *PLOS Biol.* (in press)
Boot, M. J., Westerberg, C. H., Sanz-Ezquerro, J., Cotterell, J., Schweitzer, R., Torres, M. and Sharpe, J. (2008). In vitro whole-organ imaging: 4D quantification of growing mouse limb buds. *Nat. Methods* **5**, 609-612.
Chaube, S. (1959). On axiation and symmetry in transplanted wing of the chick. *J. Exp. Zool.* **140**, 29-77.
Ciruna, B. G., Schwartz, L., Harpal, K., Yamaguchi, T. P. and Rossant, J. (1997). Chimeric analysis of fibroblast growth factor receptor-1 (Fgfr1) function: a role for FGFR1 in morphogenetic movement through the primitive streak. *Development* **124**, 2829-2841.
Cooper, M. S., Szeto, D. P., Sommers-Herivel, G., Topczewski, J., Solnica-Krezel, L., Kang, H. C., Johnson, I. and Kimelman, D. (2005). Visualizing morphogenesis in transgenic zebrafish embryos using BODIPY TR methyl ester dye as a vital counterstain for GFP. *Dev. Dyn.* **232**, 359-368.
Crossley, P. H. and Martin, G. R. (1995). The mouse Fgf8 gene encodes a family of polypeptides and is expressed in regions that direct outgrowth and patterning in the developing embryo. *Development* **121**, 439-451.
Cui, C., Yang, X., Chuai, M., Glazier, J. A. and Weijer, C. J. (2005). Analysis of tissue flow patterns during primitive streak formation in the chick embryo. *Dev. Biol.* **284**, 37-47.
Damon, B. J., Mezentseva, N. V., Kumaratilake, J. S., Forgacs, G. and Newman, S. A. (2008). Limb bud and flank mesoderm have distinct "physical phenotypes" that may contribute to limb budding. *Dev. Biol.* **321**, 319-330.
Fernández-Terán, M. A., Hinchliffe, J. R. and Ros, M. A. (2006). Birth and death of cells in limb development: a mapping study. *Dev. Dyn.* **235**, 2521-2537.
Gavin, B. J., McMahon, J. A. and McMahon, A. P. (1990). Expression of multiple novel Wnt-1/int-1-related genes during fetal and adult mouse development. *Genes Dev.* **4**, 2319-2332.
Hadjantonakis, A. K. and Papaioannou, V. E. (2004). Dynamic in vivo imaging and cell tracking using a histone fluorescent protein fusion in mice. *BMC Biotechnol.* **4**, 33.
Hasson, P., Del Buono, J. and Logan, M. P. (2007). Tbx5 is dispensable for forelimb outgrowth. *Development* **134**, 85-92.
He, F., Xiong, W., Yu, X., Espinoza-Lewis, R., Liu, C., Gu, S., Nishita, M., Suzuki, K., Yamada, G., Minami, Y. et al. (2008). Wnt5a regulates directional cell migration and cell proliferation via Ror2-mediated noncanonical pathway in mammalian palate development. *Development* **135**, 3871-3879.
Heintzelman, K. F., Phillips, H. M. and Davis, G. S. (1978). Liquid-tissue behavior and differential cohesiveness during chick limb budding. *J. Embryol. Exp. Morphol.* **47**, 1-15.
Helms, J., Thaller, C. and Eichele, G. (1994). Relationship between retinoic acid and sonic hedgehog, two polarizing signals in the chick wing bud. *Development* **120**, 3267-3274.
Hornbruch, A. and Wolpert, L. (1970). Cell division in the early growth and morphogenesis of the chick limb. *Nature* **226**, 764-766.
Li, S. and Muneoka, K. (1999). Cell migration and chick limb development: chemotactic action of FGF-4 and the AER. *Dev. Biol.* **211**, 335-347.
Min, H., Danilenko, D. M., Scully, S. A., Bolon, B., Ring, B. D., Tarpley, J. E., DeRose, M. and Simonet, W. S. (1998). Fgf-10 is required for both limb and lung development and exhibits striking functional similarity to Drosophila branchless. *Genes Dev.* **12**, 3156-3161.
Minguillon, C., Del Buono, J. and Logan, M. P. (2005). Tbx5 and Tbx4 are not sufficient to determine limb-specific morphologies but have common roles in initiating limb outgrowth. *Dev. Cell* **8**, 75-84.
Nabi, I. R. (1999). The polarization of the motile cell. *J. Cell Sci.* **112**, 1803-1811.
Naiche, L. A. and Papaioannou, V. E. (2003). Loss of Tbx4 blocks hindlimb development and affects vascularization and fusion of the allantois. *Development* **130**, 2681-2693.
Naiche, L. A. and Papaioannou, V. E. (2007). Tbx4 is not required for hindlimb identity or post-bud hindlimb outgrowth. *Development* **134**, 93-103.
Pauls, S., Geldmacher-Voss, B. and Campos-Ortega, J. A. (2001). A zebrafish histone variant H2A.F/Z and a transgenic H2A.F/Z:GFP fusion protein for in vivo studies of embryonic development. *Dev. Genes Evol.* **211**, 603-610.
Plusa, B., Piliszek, A., Frankenberg, S., Artus, J. and Hadjantonakis, A. K. (2008). Distinct sequential cell behaviours direct primitive endoderm formation in the mouse blastocyst. *Development* **135**, 3081-3091.
Rallis, C., Bruneau, B. G., Del Buono, J., Seidman, C. E., Seidman, J. G., Nissim, S., Tabin, C. J. and Logan, M. P. (2003). Tbx5 is required for forelimb bud formation and continued outgrowth. *Development* **130**, 2741-2751.
Rhee, J. M., Pirity, M. K., Lackan, C. S., Long, J. Z., Kondoh, G., Takeda, J. and Hadjantonakis, A. K. (2006). In vivo imaging and differential localization of lipid-modified GFP-variant fusions in embryonic stem cells and mice. *Genesis* **44**, 202-218.
Riddle, R. D., Johnson, R. L., Laufer, E. and Tabin, C. (1993). Sonic hedgehog mediates the polarizing activity of the ZPA. *Cell* **75**, 1401-1416.
Ros, M. A., Lopez-Martinez, A., Simandl, B. K., Rodriguez, C., Izpisua Belmonte, J. C., Dahn, R. and Fallon, J. F. (1996). The limb field mesoderm determines initial limb bud anteroposterior asymmetry and budding independent of sonic hedgehog or apical ectodermal gene expressions. *Development* **122**, 2319-2330.
Saunders, J. W., Jr (1948). The proximo-distal sequence of origin of the parts of the chick wing and the role of the ectoderm. *J. Exp. Zool.* **108**, 363-403.
Saxton, T. M., Ciruna, B. G., Holmyard, D., Kulkarni, S., Harpal, K., Rossant, J. and Pawson, T. (2000). The SH2 tyrosine phosphatase shp2 is required for mammalian limb development. *Nat. Genet.* **24**, 420-423.
Searls, R. L. and Janners, M. Y. (1971). The initiation of limb bud outgrowth in the embryonic chick. *Dev. Biol.* **24**, 198-213.
Sekine, K., Ohuchi, H., Fujiwara, M., Yamasaki, M., Yoshizawa, T., Sato, T., Yagishita, N., Matsui, D., Koga, Y., Itoh, N. et al. (1999). Fgf10 is essential for limb and lung formation. *Nat. Genet.* **21**, 138-141.
Summerhurst, K., Stark, M., Sharpe, J., Davidson, D. and Murphy, P. (2008). 3D representation of Wnt and Frizzled gene expression patterns in the mouse embryo at embryonic day 11.5 (Ts19). *Gene Expr. Patterns* **8**, 331-348.
Sun, X., Mariani, F. V. and Martin, G. R. (2002). Functions of FGF signalling from the apical ectodermal ridge in limb development. *Nature* **418**, 501-508.
Sweetman, D., Wagstaff, L., Cooper, O., Weijer, C. and Munsterberg, A. (2008). The migration of paraxial and lateral plate mesoderm cells emerging from the late primitive streak is controlled by different Wnt signals. *BMC Dev. Biol.* **8**, 63.
Vargesson, N., Clarke, J. D., Vincent, K., Coles, C., Wolpert, L. and Tickle, C. (1997). Cell fate in the chick limb bud and relationship to gene expression. *Development* **124**, 1909-1918.
Voiculescu, O., Bertocchini, F., Wolpert, L., Keller, R. E. and Stern, C. D. (2007). The amniote primitive streak is defined by epithelial cell intercalation before gastrulation. *Nature* **449**, 1049-1052.
Witze, E. S., Litman, E. S., Argast, G. M., Moon, R. T. and Ahn, N. G. (2008). Wnt5a control of cell polarity and directional movement by polarized redistribution of adhesion receptors. *Science* **320**, 365-369.
Yamaguchi, T. P., Bradley, A., McMahon, A. P. and Jones, S. (1999). A Wnt5a pathway underlies outgrowth of multiple structures in the vertebrate embryo. *Development* **126**, 1211-1223.
Zhao, X., Sirbu, I. O., Mic, F. A., Molotkova, N., Molotkov, A., Kumar, S. and Duester, G. (2009). Retinoic acid promotes limb induction through effects on body axis extension but is unnecessary for limb patterning. *Curr. Biol.* **19**, 1050-1057.